IEEE Access
Multidisciplinary | Rapid Review | Open Access Journal

Received 3 July 2023, accepted 13 July 2023, date of publication 18 July 2023, date of current version 24 July 2023.

Digital Object Identifier 10.1109/ACCESS.2023.3296498

RESEARCH ARTICLE

A Three Phase Voltage Restorer Based on Bipolar Direct AC/AC Converters

WANG YIBO, (Member, IEEE), ZHANG XINYI, LIU CHUANG, (Member, IEEE), CAI GUOWEI, LIU YU, LIU KAIPU, AND WANG YUAN

Key Laboratory of Modern Power System Simulation and Control and Renewable Energy Technology, Northeast Electric Power University, Jilin City 132012, China

Corresponding author: Wang Yibo (wangyibofangyuan@126.com)

This work was supported in part by the National Natural Science Foundation of China under Grant 52107182, and in part by the Northeast Electric Power University under Grant BSJXM-2021103.

ABSTRACT A new topology is proposed to regulate voltage sags/swells in the distribution network in this paper. Voltage sags and swells are a serious power quality problem faced by the power industry. Based on energy storage devices, the major traditional voltage restorer is not adequate for compensating deep and long-duration voltage sags/swells. To solve this problem, a novel bipolar direct AC/AC type voltage restorer (AC/AC-VR) topology is proposed, with bipolar regulation ability and no storage device. The restorer of each phase is connected to the other two phases and the power is tapped from them. By controlling the duty cycle of each AC/AC converter, the required voltage is realized to maintain stability. Analysis, simulation, and experimental results are presented to demonstrate the proposed topology.

INDEX TERMS Distribution network, voltage sag/swell, voltage restorer, bipolar direct AC/AC converter, amplitude, phase angle control.

NOMENCLATURE

U_{La}, U_{Lb}, U_{Lc}	Load voltage.
U_{SA}, U_{SB}, U_{SC}	PCC voltage.
ΔU_a, ΔU_b, ΔU_c	Voltage provided by AC/AC-VR.
U_{Saob}, U_{Saoc}	Output voltages of the direct AC/AC converter units that running in phase-A.
U_{Sboa}, U_{Sboc}	Output voltages of the direct AC/AC converter units that running in phase-B.
U_{Scoa}, U_{Scob}	Output voltages of the direct AC/AC converter units that running in phase-C.
D_{ab}, D_{ac}	Duty ratios of the phase-A AC chopper.
D_{ab}, D_{ac}	Duty ratios of the phase-B AC chopper.
D_{ab}, D_{ac}	Duty ratios of the phase-C AC chopper.
n_T	Transformation ratio of the isolated transformer.
$U_{bO1}(t)$, $U_{bO2}(t)$	Terminal voltages of P-Leg and N-Leg respectively.
d_1, d_2	Duty cycle of P-Leg and N-Leg respectively.
δ_a, δ_b, δ_c	Control angle of each phase.
M_a, M_b, M_c	Voltage amplitude regulation coefficient of each phase.

The associate editor coordinating the review of this manuscript and approving it for publication was Chandan Kumar.

I. INTRODUCTION

With the continuous popularity of various complex and precise equipment, the demand for power quality by power users is increasing. As one of the important indicators of power quality, voltage can effectively reflect the operating status and management level of the power system [1], [2]. During the operation of the power system, dynamic changes in load, switching of switch devices such as circuit breakers, and severe weather may cause undesirable voltage phenomena in the system, such as voltage sag/swell, interruptions, imbalances, and flickers. Among the numerous fluctuations in voltage, voltage sag has the greatest impact on the equipment.

This work is licensed under a Creative Commons Attribution-NonCommercial-NoDerivatives 4.0 License.
For more information, see https://creativecommons.org/licenses/by-nc-nd/4.0/

Analyze the impact of voltage sag on equipment. The results show that when the equipment is in a voltage sag state, it will affect the normal operation of the equipment, resulting in a decrease in product quality and other impacts. If the equipment is in this state for a long time, it is likely to shorten the service life of the electrical equipment or even cause damage to the electrical equipment. If the situation is serious, it will affect the production and life of social industry, bring great harm to industrial manufacturing, and bring huge losses to enterprises, such as precision mechanical tools, medical systems, and other industrial computers that rely on good voltage quality. It can be seen that voltage fluctuations can have a huge impact on production and daily life, and alleviating voltage fluctuations in the power system is an urgent problem that needs to be solved in the current power system [3], [20]. Using power devices with voltage regulation capabilities to deal with voltage sag/swell is one of the most effective methods to solve the above problems [4], [5].

Traditional voltage control methods include on-load voltage regulating transformers, static reactive power compensators, line series capacitor electrical components, etc. Figure 1 shows the Information Technology Industry Council (ITIC) curve [22]. It illustrates an acceptable power quality range. A common traditional voltage-regulating device that conforms to this curve is an on-load tap-changing transformer [23]. It can adjust the tap changer without cutting off the power supply, achieving the purpose of voltage regulation with the load. But limited by the tap changer, it cannot continuously regulate the voltage. Series capacitors regulate voltage by changing grid parameters, but they cannot adjust their own parameters with voltage fluctuations. At the same time, the series capacitor of the line is also prone to resonance in the system, bringing greater harm to the power system. Compared to the above two methods, the static reactive power compensator can quickly compensate for both inductive and capacitive reactive power simultaneously. But its output power is proportional to the square of the voltage, and when the voltage is low, the output of the static reactive power compensator is limited. Given the shortcomings of the above voltage regulation methods, the voltage restorer (VR) has attracted widespread attention from scholars because it has advantages such as regulating the voltage continuously and not bringing resonance to the system [6], [7]. In recent years, scholars around the world have done a lot of research on topology, control strategy, and optimization design of VR [8], [9], [10], [11]. Currently, the research on VR can be divided into two categories: VR based on voltage source inverters (VSI-VR) [12] and VR based on direct AC/AC conversion (AC/AC-VR) [13]. And the former can be further classified into two categories, energy storage VR and non-energy storage VR, depending on the existence of energy storage devices (e.g. capacitor, battery, etc.). Restricted by factors such as the capacity of the energy storage system, it is difficult to achieve a longer time and deeper voltage compensation in VR with the energy storage system. Furthermore, due to the existence

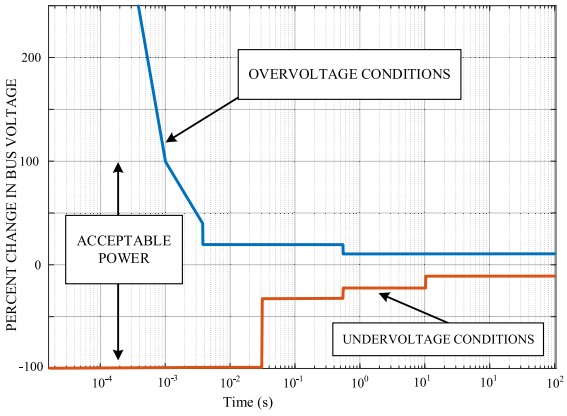

FIGURE 1. Schematic diagram of the proposed three-phase AC/AC-VR.

of energy storage system devices, such VR devices are relatively heavy and expensive. For the VR without an energy storage system, due to the addition of an AC/DC conversion system, its power has multi-level conversion, which leads to an increase in the power loss of the entire system [12], [13].

To overcome the shortcomings of the VSI-VR, AC/AC-VR is an alternative [14], [15], [16], [17]. Compared with VSI-VR, without DC-link and capacitor banks, the volume and the weight of the AC/AC-VR system have been reduced. However, for different AC/AC-VRs, given the differences in topologies and control strategies, their pros and cons are different in the operation process. For example, the AC bidirectional voltage blocking switch used in [18] makes its conversion system have commutation problems, and to effectively deal with the problem, a large and lossy resistance-capacitance (RC) buffer needs to be installed. Nevertheless, the efficiency of the conversion system is reduced. From another point of view, the commutation problem can be solved by using the improvement of the converter control strategy, but this method increases the complexity of the control process of the converter system, meanwhile, when the input/output voltage and current are highly distorted, the commutation problem is still difficult to effectively guarantee. Considering that the voltage balance of the flying capacitor has an important impact on the safe and stable operation of the converter and the operating efficiency, [19] needs to ensure that the blocking voltage of the device does not exceed its rated value during the design process. However, with the increase of the level, the balance control difficulty of the flying capacitor increases sharply [7]. And considering that voltage sag is the main cause of voltage quality problems in the distribution system, the AC/AC-VR proposed in [7] does not fully consider the voltage swell problem, that is, the implementation of bipolar compensation of the VR needs to be solved urgently.

Through the above analysis, the AC/AC converter topology proposed in the literature [21] can effectively solve the problems of commutation, flyover capacitor voltage balance,

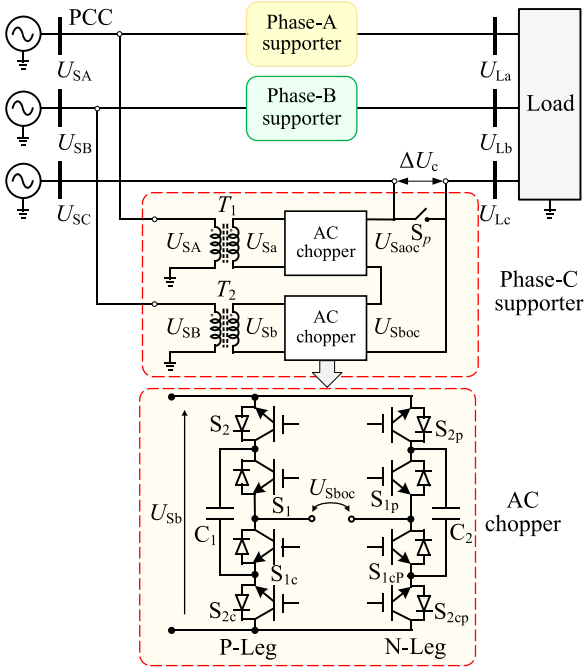

FIGURE 2. Schematic diagram of the proposed three-phase AC/AC-VR.

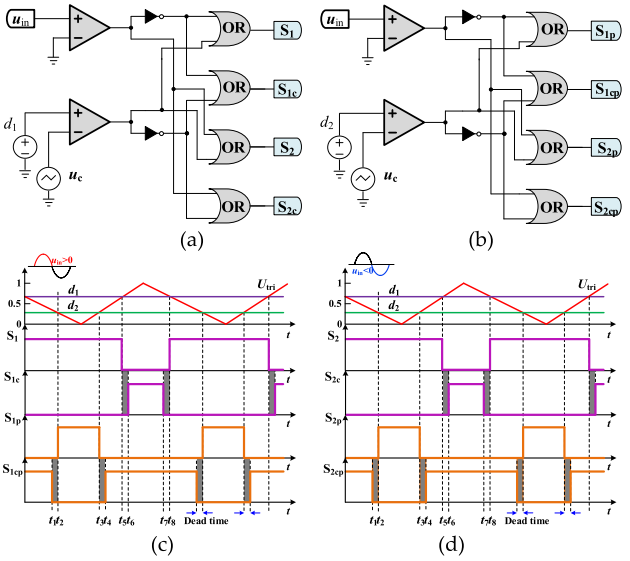

FIGURE 3. Modulation strategy of bipolar direct AC/AC converter: (a) P-leg modulation principle; (b) N-leg modulation principle; (c) P-Leg switch signal; (d) N-Leg switch signal.

and bipolar implementation in VR based on direct AC/AC converters. This topology consists of two undifferentiated PWM-type AC chopper bridge arms. It can flexibly regulate the voltage of the output port by adjusting the duty cycle of the power electronic switching devices of the 2 bridge arms, thereby achieving voltage amplitude bipolar control. This AC/AC converter not only has common ground characteristics but also does not have commutation problems during its operation. In response to the aforementioned issues and the advantages of the direct AC/AC converter proposed in the literature [21], a new topology of three-phase AC/AC-VR based on bipolar direct AC/AC converter is proposed in this paper and the rest of the paper is organized as follows. In Section II, the topology, voltage regulation range, and control strategy proposed in this paper are introduced; In Section III, the results obtained by the method proposed in this paper are discussed and analyzed; Conclusions are drawn in Section IV.

II. METHODOLOGY

A. PROPOSED TOPOLOGY OF THE THREE-PHASE AC/AC-VR

The schematic diagram of the proposed topology for the three-phase AC/AC-VR with a detailed phase-C supporter is illustrated in Figure 2. The proposed three-phase AC/AC-VR is composed of three supporter modules, each of which works on phases-A, phases-B, and phases-C, respectively. As shown in Figure 2, each phase circuit topology includes a voltage regulator module, which is connected in series between the power grid and the load. Each module contains two AC/AC converters, two transformers T_1 and T_2, and a bypass switch S_p. Transformers T_1 and T_2 are isolation transformers with the function of galvanic isolation. The AC/AC converter is mainly composed of power electronic devices, which play a role in regulating voltage in AC/AC-VR. Analyze the topology structure, and it shows that the input ports of isolation transformers T_1 and T_2 are connected in series with the A phase circuit and the B phase circuit, respectively, and the output port is connected to the input port of the AC/AC converter. The transformation ratio of the isolation transformer is n_T. Two AC/AC converter output ports are connected in series, and the voltage output by the two is connected in series with the load voltage. As a result, the C-phase load voltage has been effectively regulated. When the point of common coupling (PCC) voltage U_{SA}, U_{SB}, and U_{SC} sags/swells, the load voltage U_{La}, U_{Lb}, and U_{Lc} can be maintained through AC/AC-VR. At this time, the voltage it provides is ΔU_a, ΔU_b, ΔU_c. That is, the voltage relationship obtained as follows:

$$\begin{cases} U_{La}(t) = U_{SA}(t) - \Delta U_a(t) \\ U_{Lb}(t) = U_{SB}(t) - \Delta U_b(t) \\ U_{Lc}(t) = U_{SC}(t) - \Delta U_c(t) \end{cases} \tag{1}$$

Furthermore, each supporter is supported by the other two phases, i.e., phase-C supporter works on phase-C, and its compensation voltage ΔU_c is supported by phase-A and phase-B. In addition, the other two phases are similar, and follow the following formula:

$$\begin{cases} \Delta U_a(t) = U_{Sboa}(t) + U_{Scoa}(t) \\ \Delta U_b(t) = U_{Scob}(t) + U_{Saob}(t) \\ \Delta U_c(t) = U_{Saoc}(t) + U_{Sboc}(t) \end{cases} \tag{2}$$

$$\begin{cases} U_{Sboa}(t) = D_{ab} \cdot U_{Sb}(t) \\ U_{Scoa}(t) = D_{ac} \cdot U_{Sc}(t) \\ U_{Scob}(t) = D_{bc} \cdot U_{Sc}(t) \\ U_{Saob}(t) = D_{ba} \cdot U_{Sa}(t) \\ U_{Saoc}(t) = D_{ca} \cdot U_{Sa}(t) \\ U_{Sboc}(t) = D_{cb} \cdot U_{Sb}(t) \end{cases} \tag{3}$$

$$\begin{cases} U_{Sa}(t) = \dfrac{1}{n_T} U_{SA}(t) \\ U_{Sb}(t) = \dfrac{1}{n_T} U_{SB}(t) \\ U_{Sc}(t) = \dfrac{1}{n_T} U_{SC}(t) \end{cases} \tag{4}$$

where (U_{Sboa}, U_{Scoa}), (U_{Scob}, U_{Saob}) and (U_{Saoc}, U_{Sboc}) are the output voltages of the direct AC/AC converter units that running in phase-A, phase-B, and phase-C, respectively. (D_{ab}, D_{ac}), (D_{bc}, D_{ba}) and (D_{ca}, D_{cb}) are the duty ratios of the AC chopper operating on the three phases, respectively. n_T is the transformation ratio of the isolated transformer.

B. OPERATING MODE AND VOLTAGE REGULATION RANGE

1) PWM WORKING MODE OF THE CONVERTER

As can be seen from Figure 2, the bipolar direct AC/AC converter adopted is composed of two non-differential PWM AC/AC chopper bridge arms, which are defined as P-Leg and N-Leg, respectively. And there are four IGBTs (S_1, S_{1C}, S_2, S_{2C}, and S_{1P}, S_{1cp}, S_{2p}, and S_{2cp}) and a capacitor (C_1 and C_2) for absorbing the energy in the line stray inductance in each arm. An H-bridge structure is constituted evidently. Further, P-Leg and N-Leg have the same modulation principle shown in Figure 3.

As shown in Figure 3, u_c is a triangular carrier with a scope value of 0 to 1. According to the PWM modulation principle: regardless of the polarity of the converter input voltage, in each half cycle, 4 of the 8 IGBTs of P-Leg and N-Leg are always normally open and 4 receive modulation for high-frequency action, that is, the converter has up to 4 IGBTs for high-frequency action, and the switching loss is effectively reduced. On the other hand, the output voltage polarity of the converter is directly related to the input voltage polarity. The output voltage of the converter has the following relationship with the input voltage:

$$U_{Sboc}(t) = U_{bO1}(t) - U_{bO2}(t) = (d_1 - d_2) \cdot U_{Sb}(t) \tag{5}$$

where $U_{bO1}(t)$ and $U_{bO2}(t)$ are the terminal voltages of P-Leg and N-Leg respectively; d_1 and d_2 are the duty cycle of P-Leg and N-Leg respectively, and their value range is [0,1].

According to the previous analysis, the output voltage of the converter can be regulated by adjusting the values of d_1 and d_2, that is, the converter has a dual degree of freedom regulation ability, and the converter has high operation flexibility. Considering the value range of d_1 and d_2, it can be seen that the variation range of (d_1 - d_2) is [-1,1], that is, it has bipolar regulation ability.

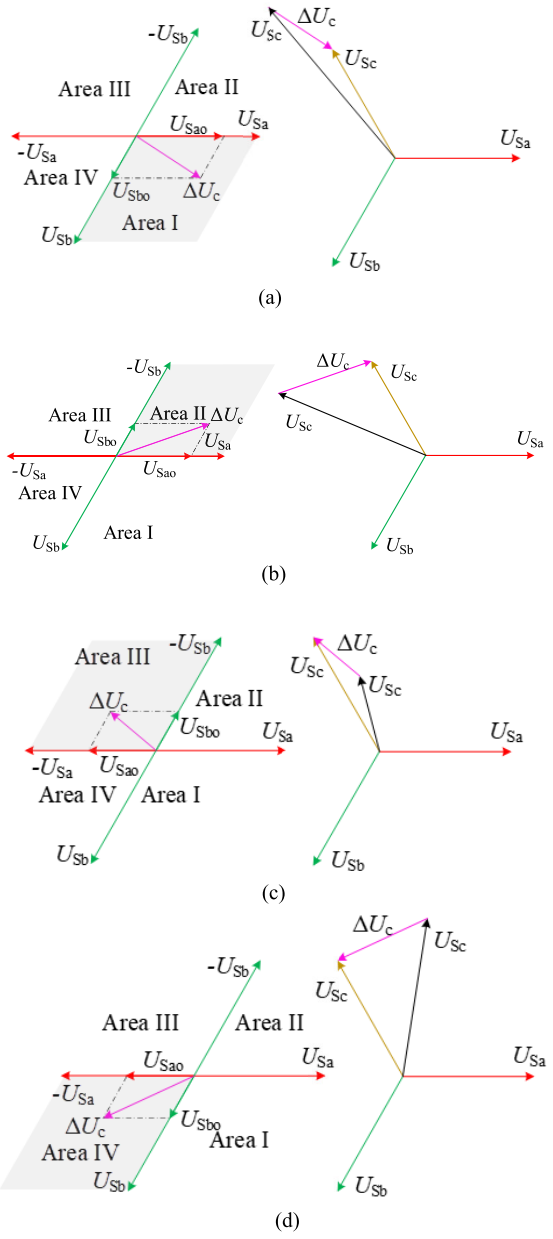

FIGURE 4. Vector diagram of operation mode of AC/AC-VR (phase-C): (a) Mode I: Dca > 0, Dcb > 0; (b) Mode II: Dca > 0, Dcb < 0. (c) Mode III: Dca < 0, Dcb < 0; (d) Mode IV: Dca < 0, Dcb > 0.

2) VOLTAGE REGULATION RANGE

The voltage compensation capacity of AC/AC-VR can be calculated by (6). Furthermore, it is determined by the duty cycle (D_{ab}, D_{ac}), (D_{bc}, D_{ba}), and (D_{ca}, D_{cb}).

$$\begin{cases} \Delta U_a(t) = D_{ab} \cdot \dfrac{1}{n_T} U_{SB}(t) + D_{ac} \cdot \dfrac{1}{n_T} U_{SC}(t) \\ \Delta U_b(t) = D_{bc} \cdot \dfrac{1}{n_T} U_{SC}(t) + D_{ba} \cdot \dfrac{1}{n_T} U_{SA}(t) \\ \Delta U_c(t) = D_{ca} \cdot \dfrac{1}{n_T} U_{SA}(t) + D_{cb} \cdot \dfrac{1}{n_T} U_{SB}(t) \end{cases} \tag{6}$$

To sum up, the operation mode of the proposed three-phase AC/AC-VR can be represented by phase-C in Figure 4., and

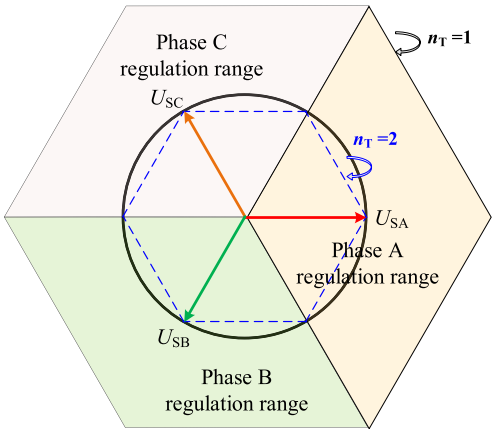

FIGURE 5. Voltage regulation range of AC/AC-VR.

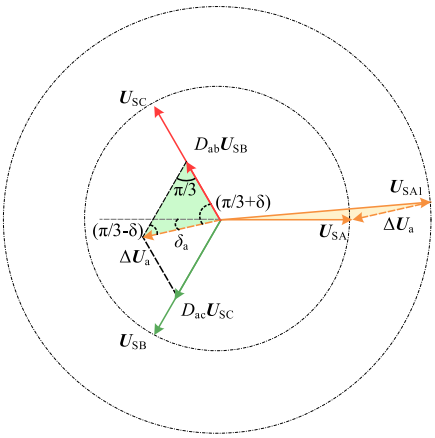

FIGURE 6. Regulation principle diagram of phase-A.

when the AC choppers used in AC/AC-VR are bipolar converters, AC/AC-VR has the following I-IV operation mode, otherwise, there is only the I mode, i.e., with bipolar direct AC/AC converter, the AC/AC-VR has a wider regulation range.

The AC/AC converter adopted in this paper has bipolar regulation characteristics, and the duty cycle value range is [-1, 1], thus, the maximum value of the voltage regulation range can be calculated by (7).

$$\begin{cases} \Delta U_a(t) = \dfrac{\pm 1}{n_T} U_{SB}(t) + \dfrac{\pm 1}{n_T} U_{SC}(t) \\ \Delta U_b(t) = \dfrac{\pm 1}{n_T} U_{SC}(t) + \dfrac{\pm 1}{n_T} U_{SA}(t) \\ \Delta U_c(t) = \dfrac{\pm 1}{n_T} U_{SA}(t) + \dfrac{\pm 1}{n_T} U_{SB}(t) \end{cases} \tag{7}$$

According to equation (7), when the value of the isolation transformer turns ratio n_T is different, the voltage regulation range of AC/AC-VR is diverse either, i.e., the voltage regulation range of the AC/AC-VR is related to the turn ratio n_T. The voltage regulation range with different turns ratio n_T is shown in Figure 5.

As shown in Figure 5, considering the actual operating scenario, generally $n_T \geq 1$. When $D_{ab} = D_{ac}$, $D_{bc} = D_{ba}$, and $D_{ca} = D_{cb}$, AC/AC-VR can only regulate the amplitude of the output side voltage. And when $n_T = 1$, AC/AC-VR can regulate 100% voltage swell and sag. When $D_{ab} \neq D_{ac}$, $D_{bc} \neq D_{ba}$, and $D_{ca} \neq D_{cb}$, AC/AC-VR can independently adjust the phase angle and amplitude of the output side voltage simultaneously. As shown in the figure, as the n_T value increases, the adjustable voltage range of AC/AC-VR output decreases, that is, the adjustable range of AC/AC-VR decreases. Therefore, in practical applications, an appropriate n_T can be selected based on the required voltage regulation range and other factors.

C. CONTROL STRATEGY

Based on the above theoretical analysis, a control strategy for AC/AC-VR system is proposed. And for ease of illustration, take phase-A as an example to draw the AC/AC-VR voltage regulation schematic diagram, as shown in Figure 6.

Figure 6 illustrates that the AC/AC-VR system needs to provide a compensation voltage ΔU_a for phase-A when the phase-A voltage swells from U_{SA} to U_{SA1}. And the regulated voltage ΔU_a is synthesized by the output voltages (U_{Sboa}, U_{Scoa}) of two bipolar direct AC/AC converter units operating on phase-A. Based on the triangle edge angle theory, the following relationship is satisfied in the voltage regulation process.

$$\frac{\Delta U_a}{\sin(\pi/3)} = \frac{D_{ab} \cdot U_{SB}}{\sin(\pi/3 + \theta_a)} = \frac{D_{ac} \cdot U_{SC}}{\sin(\pi/3 - \theta_a)} \tag{8}$$

Further, in a three-phase system:

$$\begin{cases} \dfrac{\Delta U_a}{\sin(\pi/3)} = \dfrac{D_{ab} \cdot U_{SB}}{\sin(\pi/3 + \theta_a)} = \dfrac{D_{ac} \cdot U_{SC}}{\sin(\pi/3 - \theta_a)} \\ \dfrac{\Delta U_b}{\sin(\pi/3)} = \dfrac{D_{bc} \cdot U_{SC}}{\sin(\pi/3 + \theta_b)} = \dfrac{D_{ba} \cdot U_{SA}}{\sin(\pi/3 - \theta_b)} \\ \dfrac{\Delta U_c}{\sin(\pi/3)} = \dfrac{D_{ca} \cdot U_{SA}}{\sin(\pi/3 + \theta_c)} = \dfrac{D_{cb} \cdot U_{SB}}{\sin(\pi/3 - \theta_c)} \end{cases} \tag{9}$$

On the other hand, formula (10) can be derived from formula (2) and formula (9):

$$\begin{cases} U_{La}(t) = U_{SA} \angle(\omega t) + \sqrt{2} M_a \cdot U_{SA} \angle(\omega t + \theta_a) \\ U_{Lb}(t) = U_{SB} \angle(\omega t) + \sqrt{2} M_b \cdot U_{SB} \angle(\omega t + \theta_b) \\ U_{Lc}(t) = U_{SC} \angle(\omega t) + \sqrt{2} M_c \cdot U_{SC} \angle(\omega t + \theta_c) \end{cases} \tag{10}$$

Which

$$\begin{cases} M_a = \dfrac{1}{2n} \sqrt{(D_{ab} + D_{ac})^2 + 3(D_{ab} - D_{ac})^2} \\ M_b = \dfrac{1}{2n} \sqrt{(D_{bc} + D_{ba})^2 + 3(D_{bc} - D_{ba})^2} \\ M_c = \dfrac{1}{2n} \sqrt{(D_{ca} + D_{cb})^2 + 3(D_{ca} - D_{cb})^2} \end{cases} \tag{11}$$

$$\begin{cases} \theta_a = \tan^{-1}\left[\sqrt{3}(D_{ab} - D_{ac}) \Big/ (D_{ab} + D_{ac})\right] \\ \theta_b = \tan^{-1}\left[\sqrt{3}(D_{bc} - D_{ba}) \Big/ (D_{bc} + D_{ba})\right] \\ \theta_c = \tan^{-1}\left[\sqrt{3}(D_{ca} - D_{cb}) \Big/ (D_{ca} + D_{cb})\right] \end{cases} \tag{12}$$

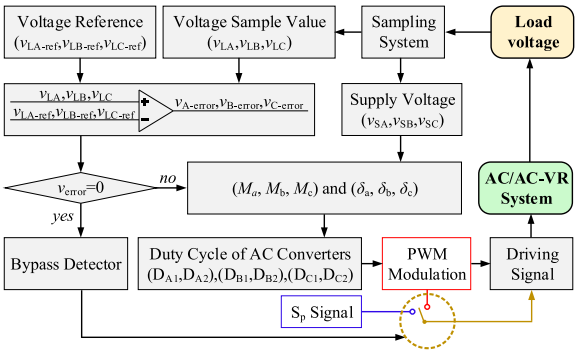

FIGURE 7. AC/AC-VR system control block diagram.

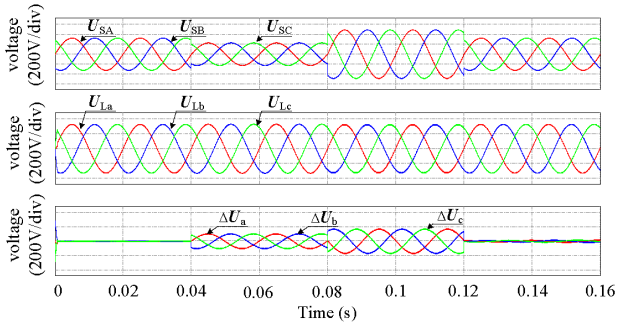

FIGURE 8. Simulation results of voltage amplitude regulation.

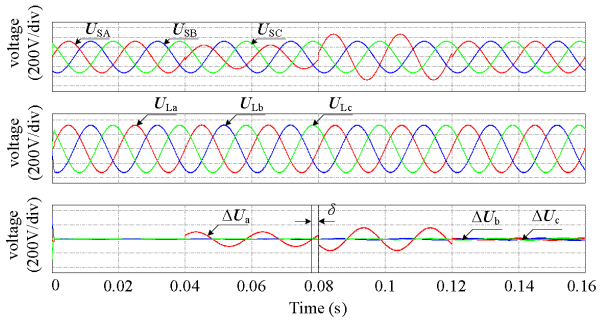

FIGURE 9. Simulation results of voltage amplitude and phase angle regulation.

From the above analysis, it can be seen that when $D_{ab} = D_{ac}$, $D_{bc} = D_{ba}$, $D_{ca} = D_{cb}$, the AC/AC-VR system can realize the flexible regulation of the voltage amplitude only, i.e., $\delta_a = \delta_b = \delta_c = 0$. Otherwise, the AC/AC-VR system can realize the simultaneous regulation of voltage amplitude and phase angle. Then, the control block diagram of the AC/AC-VR system can be presented in Figure 7.

In Figure 7, the bypass switch S_p is turned on when the system voltage is stable or the AC/AC-VR fails, and the AC/AC-VR exits operation. When the sampling detection system detects a change in the grid voltage (swells or sags), the AC/AC-VR is activated. Voltage amplitude and phase angle are regulated by comparing the sample value with the target value to achieve voltage stability regulation.

III. RESULTS AND DISCUSSION

A. SIMULATION RESULTS

To verify the correctness and effectiveness of the proposed AC/AC-VR, a 380 V low-voltage simulation platform is built. The simulation conditions are as follows: the turn ratio of the isolation transformer is $n_T = 2$, a three-phase voltage amplitude sag with a depth of 0.3p.u. occurs from 0.04s to 0.08s, and from 0.08s to 0.12s, the amplitude of three-phase voltage with a depth of 0.5p.u. swell, and the voltage returned to normal at 0.12s. The simulation result is shown in Figure 8.

As can be seen from Figure 8, from 0s to 0.04s, the grid voltage U_{SA}, $U_{SB,}$ and U_{SC} remain stable, the load voltage U_{La}, $U_{Lb,}$ and U_{Lc} are equal to the grid voltage, and the output voltage of AC/AC-VR equal to zero, i.e. it during standby mode. At 0.04s, grid voltage amplitude sag, to maintain the stability of load voltage, regulated voltage ΔU_a, ΔU_b, ΔU_c are provided by AC/AC-VR, i.e. it is injection mode (during sag). At 0.08s, U_{SA}, $U_{SB,}$ and U_{SC} turn from sag to swell, and AC/AC-VR provides reverse regulation voltage to meet the needs of the load, i.e. it is in injection mode (during swell). At 0.12s, U_{SA}, $U_{SB,}$ and U_{SC} return to normal, and the compensation voltage of AC/AC-VR turns to zero again. In the whole dynamic simulation process, U_{La}, $U_{Lb,}$ and U_{Lc} remain stable, i.e. it return to the standby mode.

Further, to verify and analyze the compensation effect of the proposed AC/AC-VR under the scenario of asymmetric sag/swell of grid voltage, the following simulation conditions are given: single phase voltage sag, 0.3p.u., with phase angle jump, $\delta = 30^{\circ}$, during [0.04s, 0.08s]. And during [0.08s, 0.12s], single phase voltage swell, 0.5p.u., with phase angle jump, $\delta = 30^{\circ}$. Then, the voltage returns to normal at 0.12s, and the simulation results are shown in Figure 9

Similarly, as can be seen from Figure 9, during [0s, 0.04s] and [0.12s, 0.16s], the grid voltage U_{SA}, $U_{SB,}$ and U_{SC} remains constant and equal to the load voltage U_{La}, U_{Lb} and U_{Lc}, naturally, AC/AC-VR provides zero voltage, i.e. it during standby mode. During [0.04s, 0.08s] and [0.08, 0.12s], voltage sag/swell with phase angle jump appeared respectively, at this point, compensation voltage is provided by AC/AC-VR, i.e. it is injection mode. To sum up, the simulation results are consistent with expectations in the differentiated scenario.

B. EXPERIMENTAL RESULTS

In this section, to examine the compensation capability of the control method and the proposed topology, an experimental prototype of this device according to Figure 2 is implemented. The applied system parameters in the experimental cases are presented as shown in Table 1. Limited to laboratory conditions and to facilitate the experiment, only A-phase is taken as an example to conduct an open-loop experiment on the performance of AC/AC-VR. Meanwhile, the B-phase and C-phase of AC/AC-VR are taken from the secondary side of the three-phase voltage regulating

TABLE 1. Experimental parameters of AC/AC-VR system.

IGBT	IKW75N60T
U_{Sa}	110V
n_T	2:1
Sampling frequency	10 kHz
Switching frequency	10 kHz
Filter inductance L_f	0.3 mH
Filter capacitor C_f	10 μF

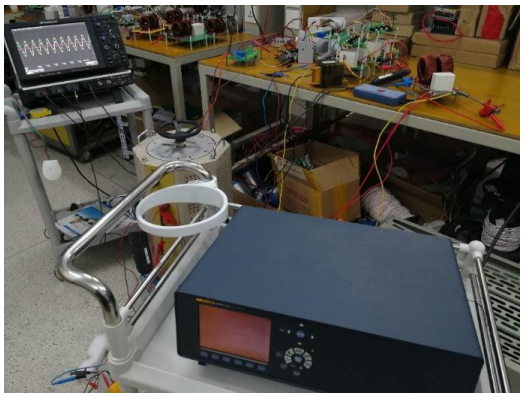

FIGURE 10. Schematic diagram of the experimental platform.

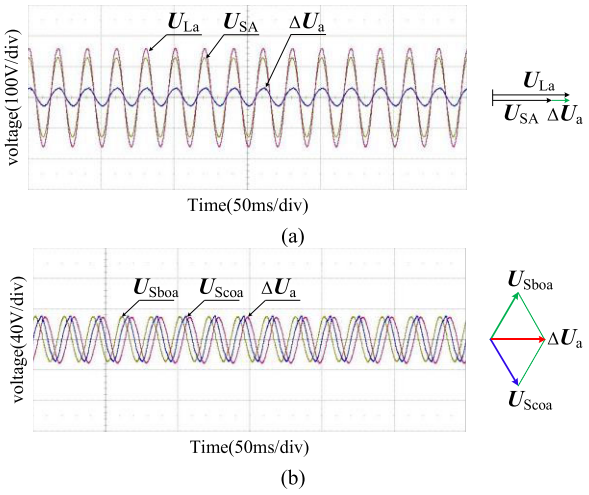

FIGURE 11. Experimental results of voltage amplitude regulation: (a) U_{La}, U_{SA}, and ΔU_a experimental waveforms; (b) U_{Sboa}, U_{Scoa}, and ΔU_a experimental waveforms.

transformer, and its transformation ratio is 2:1. Two scenarios are selected for analysis in the experiment: voltage amplitude sag depth of 0.2p.u. and voltage phase angle offset of 25°. The schematic diagram of the experimental platform and experimental results are shown in Figure 11 and Figure 12, respectively.

As shown in Figure 11(a), an experimental waveform diagram of load voltage U_{La}, power side voltage U_{SA} and compensation voltage ΔU_a is obtained. It can be seen that when the voltage amplitude of the A-phase sags and is lower

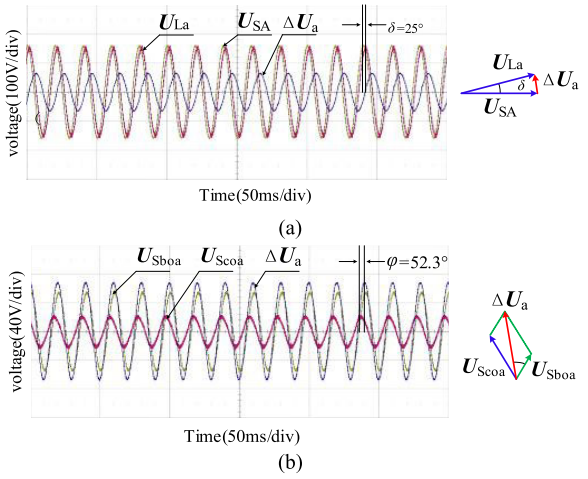

FIGURE 12. Experimental results of voltage amplitude and phase angle regulation: (a) U_{La}, U_{SA}, and ΔU_a experimental waveforms; (b) U_{Sboa}, U_{Scoa}, and ΔU_a experimental waveforms.

than the load required, the compensation voltage provided by B-phase and C-phase correspondingly. And it can be seen that the combined voltage provided by B-phase and C-phase is in-phase with A-phase. Figure 11 (b) shows the experimental waveforms of B-phase and C-phase output voltages; meanwhile, synthetic voltage, i.e., compensation voltage ΔU_a is provided by AC/AC-VR. At this time, the voltage amplitude of the B-phase and C-phase is equal, and the phase angle difference is 120 degrees. To sum up, the provided AC/AC-VR can effectively maintain the load voltage stability.

Similarly, an experimental waveform diagram of load voltage U_{La}, power side voltage U_{SA} and compensation voltage ΔU_a is shown in Figure 12(a), as can be seen from the figure that the voltage on the power side is offset by a phase angle of $\delta = 25^\circ$. At this point, AC/AC-VR provided a compensation voltage to keep the load voltage unchanged. And there is an angle between the compensation voltage ΔU_a and the supply voltage U_{SA}. And the voltage synthesis process can be reflected in Figure 12(b). With 60° included angle between the B-phase and C-phase, the angles between the synthesized voltage ΔU_a and the output voltage of B-phase and C-phase are 52.3° and 7.7°, respectively.

That is, the experiment result shows that when the phase angle offset of A-phase voltage occurs, the provided AC/AC-VR can realize the effective regulation of load voltage and meet the needs of the load well.

IV. CONCLUSION

In this paper, a novel three-phase voltage restorer based on bipolar direct AC/AC converters is proposed to compensate for voltage sags/swells. The topology has many advantages such as no storage device, no commutation problems, no RC buffer, reduced size, heavy, cost, etc., and with a simple control system and voltage bipolar regulation ability. In single-phase sag/swell, energy is taken from healthy phases, without any burden on the faulty phase. The operation and control

techniques of this topology are explained in detail. In this paper, simulation and experimental verification have been conducted for voltage amplitude sag/surge scenarios and voltage regulation scenarios with phase angle jumps. Under different scenarios, the proposed DVRs proposed in this paper have good voltage compensation effects and meet the load voltage requirements.

In future research, the different control strategies of AC/AC-VR and their corresponding stability will be further studied. In addition, it is also necessary to focus on the asymmetric modeling and harmonic suppression ability of AC/AC-VR. Although, as analyzed above, the proposed AC/AC-VR has many advantages. However, due to the topology of AC/AC-VR, it still has the following disadvantages. Firstly, the PCC may experience noise due to a direct AC/AC circuit. Secondly, the required power is drawn from the faulty phases in the case of symmetrical voltage sag compensation. Thirdly, the topology uses a large number of IGBTs. Finally, due to the limitations of IGBT, the voltage level of the proposed AC/AC-VR application is limited. Therefore, further optimization of the topology structure such as the connection method of AC/AC-VR isolation transformers is needed to ensure better performance of the proposed AC/AC-VR.

REFERENCES

[1] S. Hasan, K. M. Muttaqi, D. Sutanto, and Md. A. Rahman, "A novel dual slope delta modulation technique for a current source inverter based dynamic voltage restorer for mitigation of voltage sags," *IEEE Trans. Ind. Appl.*, vol. 57, no. 5, pp. 5437–5447, Sep. 2021.

[2] X. Chen, Q. Xie, X. Bian, and B. Shen, "Energy-saving superconducting magnetic energy storage (SMES) based interline DC dynamic voltage restorer," *CSEE J. Power Energy Syst.*, vol. 8, no. 1, pp. 238–248, Jan. 2022.

[3] J. Kaniewski, "Three-phase power flow controler based on bipolar AC/AC converter with matrix choppers," in *Proc. Int. Symp. Power Electron., Electr. Drives, Autom. Motion (SPEEDAM)*, Amalfi, Italy, Jun. 2018, pp. 709–715.

[4] J. Kaniewski, P. Szczesniak, and M. Jarnut, "Three-phase power flow controler with AC/AC converter based on matrix-reactance chopper," in *Proc. 9th Int. Conf. Compat. Power Electron. (CPE)*, Costa da Caparica, Portugal, Jun. 2015, pp. 210–215.

[5] J. Kaniewski, Z. Fedyczak, and G. Benysek, "AC voltage sag/swell compensator based on three-phase hybrid transformer with buck-boost matrix-reactance chopper," *IEEE Trans. Ind. Electron.*, vol. 61, no. 8, pp. 3835–3846, Aug. 2014.

[6] C. Tu, Q. Guo, F. Jiang, H. Wang, and Z. Shuai, "A comprehensive study to mitigate voltage sags and phase jumps using a dynamic voltage restorer," *IEEE J. Emerg. Sel. Topics Power Electron.*, vol. 8, no. 2, pp. 1490–1502, Jun. 2020.

[7] S. Kim, H.-G. Kim, and H. Cha, "Dynamic voltage restorer using switching cell structured multilevel AC–AC converter," *IEEE Trans. Power Electron.*, vol. 32, no. 11, pp. 8406–8418, Nov. 2017.

[8] P. Li, Y. Wang, M. Savaghebi, J. Lu, X. Pan, and F. Blaabjerg, "Identification design for dynamic voltage restorer to mitigate voltage sag based on the elliptical transformation," *IEEE J. Emerg. Sel. Topics Power Electron.*, vol. 9, no. 5, pp. 5672–5686, Oct. 2021.

[9] Q. Zhong, Q. He, G. Wang, L. Wang, and Q. Li, "Optimal sizing and placement method for dynamic voltage restorers with mitigation expectation index," *IEEE Trans. Power Del.*, vol. 36, no. 6, pp. 3561–3569, Dec. 2021.

[10] S. Majumder, S. A. Khaparde, A. P. Agalgaonkar, S. V. Kulkarni, and S. Perera, "Graph theory based voltage sag mitigation cluster formation utilizing dynamic voltage restorers in radial distribution networks," *IEEE Trans. Power Del.*, vol. 37, no. 1, pp. 18–28, Feb. 2022.

[11] P. Ghavidel, M. Farhadi, M. Dabbaghjamanesh, A. Jolfaei, and M. Sabahi, "Fault current limiter dynamic voltage restorer (FCL-DVR) with reduced number of components," *IEEE J. Emerg. Sel. Topics Ind. Electron.*, vol. 2, no. 4, pp. 526–534, Oct. 2021.

[12] J. G. Nielsen and F. Blaabjerg, "A detailed comparison of system topologies for dynamic voltage restorers," *IEEE Trans. Ind. Appl.*, vol. 41, no. 5, pp. 1272–1280, Oct. 2005.

[13] S. Subramanian and M. Kumar Mishra, "Interphase AC–AC topology for voltage sag supporter," *IEEE Trans. Power Electron.*, vol. 25, no. 2, pp. 514–518, Feb. 2010.

[14] F. Zheng Peng, L. Chen, and F. Zhang, "Simple topologies of PWM AC–AC converters," *IEEE Power Electron Lett.*, vol. 1, no. 1, pp. 10–13, Mar. 2003.

[15] S. Jothibasu and M. K. Mishra, "An improved direct AC–AC converter for voltage sag mitigation," *IEEE Trans. Ind. Electron.*, vol. 62, no. 1, pp. 21–29, Jan. 2015.

[16] S. Jothibasu and M. K. Mishra, "A control scheme for storageless DVR based on characterization of voltage sags," *IEEE Trans. Power Del.*, vol. 29, no. 5, pp. 2261–2269, Oct. 2014.

[17] J. Kaniewski, P. Szczesniak, M. Jarnut, and G. Benysek, "Hybrid voltage sag/swell compensators: A review of hybrid AC/AC converters," *IEEE Ind. Electron. Mag.*, vol. 9, no. 4, pp. 37–48, Dec. 2015.

[18] H.-H. Shin, H. Cha, H.-G. Kim, and D.-W. Yoo, "Novel single-phase PWM AC–AC converters solving commutation problem using switching cell structure and coupled inductor," *IEEE Trans. Power Electron.*, vol. 30, no. 4, pp. 2137–2147, Apr. 2015.

[19] C. Feng, J. Liang, and V. G. Agelidis, "Modified phase-shifted PWM control for flying capacitor multilevel converters," *IEEE Trans. Power Electron.*, vol. 22, no. 1, pp. 178–185, Jan. 2007.

[20] D. P. Simatupang and J. Choi, "Integrated photovoltaic inverters based on unified power quality conditioner with voltage compensation for submarine distribution system," *Energies*, vol. 11, no. 11, p. 2927, Oct. 2018.

[21] C. Liu, D. Guo, R. Shan, G. Cai, W. Ge, Z. Huang, Y. Wang, H. Zhang, and P. Wang, "Novel bipolar-type direct AC–AC converter topology based on non-differential AC choppers," *IEEE Trans. Power Electron.*, vol. 34, no. 10, pp. 9585–9599, Oct. 2019.

[22] J. Kyei, R. Ayyanar, G. Heydt, R. Thallam, and J. Blevins, "The design of power acceptability curves," *IEEE Trans. Power Del.*, vol. 17, no. 3, pp. 828–833, Jul. 2002.

[23] N. Yorino, M. Danyoshi, and M. Kitagawa, "Interaction among multiple controls in tap change under load transformers," *IEEE Trans. Power Syst.*, vol. 12, no. 1, pp. 430–436, Feb. 1997.

WANG YIBO (Member, IEEE) was born in Shandong, China, in 1989. He received the B.S., M.S., and Ph.D. degrees in electrical engineering from Northeast Electric Power University, Jilin, China, in 2010, 2016, and 2020, respectively. Since 2020, he has been a Teacher with the School of Electrical Engineering, Northeast Electric Power University. His research interests include renewable energy integration into power networks, power systems, and power quality.

ZHANG XINYI was born in Liaoning, China, in 1998. She received the B.S. degree in electrical engineering from Northeast Electric Power University, Jilin, China, in 2020, where she is currently pursuing the M.S. degree in electrical engineering. Her research interests include hybrid distribution transformer and voltage flexible regulation.

LIU CHUANG (Member, IEEE) received the M.S. degree in electrical engineering from Northeast Electric Power University, Jilin, China, in 2009, and the Ph.D. degree in electrical engineering from the Harbin Institute of Technology, Harbin, China, in 2013.

From 2010 to 2012, he was with the Future Energy Electronics Center, Virginia Polytechnic Institute and State University, Blacksburg, VA, USA, as a Visiting Ph.D. Student, supported by the Chinese Scholarship Council. In 2013, he was an Associate Professor with the School of Electrical Engineering, Northeast Electric Power University, where he has been a Professor, since 2016. His research interests include power-electronics-based on ac and dc transformers for future hybrid ac–dc power grids, flexible operation and control of power grid based on ac–ac transformation, and power-electronics-based power system stability analysis and control.

CAI GUOWEI was born in Jilin, China, in 1968. He received the B.S. and M.S. degrees in electrical engineering from Northeast Electric Power University, Jilin, in 1990 and 1993, respectively, and the Ph.D. degree in electrical engineering from the Harbin Institute of Technology, Harbin, China, in 1999. Since 2004, he has been a Professor with the School of Electrical Engineering, Northeast Electric Power University. His research interests include power system transient stability analysis and smart grid with renewable power.

LIU YU was born in Shandong, China, in 1999. He received the B.S. degree in electrical engineering from Northeast Electric Power University, Jilin, China, in 2021, where he is currently pursuing the master's degree in electrical engineering. His research interests include hybrid transformer and power quality.

LIU KAIPU was born in Shandong, China, in 2000. He received the B.S. degree in electrical engineering from Shandong Jianzhu University, Jinan, China, in 2021. He is currently pursuing the master's degree in electrical engineering with Northeast Electric Power University. His research interests include hybrid transformer and flexible regulation of distribution networks.

WANG YUAN was born in Henan, China, in 1999. He received the B.S. degree in electrical engineering from Henan Polytechnic University, Henan, in 2021. He is currently pursuing the master's degree in electrical engineering with Northeast Electric Power University. His research interests include hybrid transformer and power quality.